

The QCD heavy-quark potential to order v^2 : one loop matching conditions

Aneesh V. Manohar* and Iain W. Stewart†

Department of Physics, University of California at San Diego,
9500 Gilman Drive, La Jolla, CA 92093

Abstract

The one-loop QCD heavy quark potential is computed to order v^2 in the color singlet and octet channels. Several errors in the previous literature are corrected. To be consistent with the velocity power counting, the full dependence on $|\mathbf{p} + \mathbf{p}'|/|\mathbf{p}' - \mathbf{p}|$ is kept. The matching conditions for the NRQCD one-loop potential are computed by comparing the QCD calculation with that in the effective theory. The graphs in the effective theory are also compared to terms from the hard, soft, potential, and ultrasoft regimes in the threshold expansion. The issue of off-shell versus on-shell matching and gauge dependence is discussed in detail for the $1/(m|\mathbf{k}|)$ term in the potential. Matching on-shell gives a $1/(m|\mathbf{k}|)$ potential that is gauge independent and does not vanish for QED.

Typeset using REVTeX

*amanohar@ucsd.edu

†iain@schwinger.ucsd.edu

I. INTRODUCTION

For processes involving a non-relativistic heavy quark and antiquark, it is useful to combine the α_s expansion of QCD with an expansion in powers of the relative velocity v . The scattering of a heavy quark and antiquark, $Q(\mathbf{p}) + \bar{Q}(-\mathbf{p}) \rightarrow Q(\mathbf{p}') + \bar{Q}(-\mathbf{p}')$, can be described using a potential V , which has an expansion in powers of the velocity v and α_s ,

$$V(\mathbf{p}, \mathbf{p}') = \sum_{n=-2}^{\infty} V^{(n)}, \quad V^{(n)} = \sum_{j=1}^{\infty} V^{(n,j)},$$

where $V^{(n)} \sim v^n$, $V^{(n,j)} \sim v^n \alpha_s^j$. (1)

An important complication of non-relativistic scattering is the presence of two low-energy scales, mv and mv^2 , which correspond to the momentum and energy of the heavy quark, respectively. In this paper, we will assume that $mv^2 \gg \Lambda_{\text{QCD}}$, and ignore any non-perturbative effects.

The first term in Eq. (1), $V^{(-2,1)}$, is the static Coulomb potential at tree-level,

$$V^{(-2,1)} = C \frac{4\pi\alpha_s}{|\mathbf{p} - \mathbf{p}'|^2}, \quad (2)$$

where the color factor C depends on the relative color state of the incident quark and antiquark. For $j > 1$, $V^{(-2,j)}$ are perturbative corrections to the Coulomb potential which are known to two loops [1,2].

The static potential for a color singlet $Q\bar{Q}$ pair is often defined in terms of the expectation value of a rectangular Wilson loop of width R and length T :

$$V^{(-2)}(R) = - \lim_{T \rightarrow \infty} \frac{1}{iT} \ln \left\langle \text{Tr } P \exp \left(ig \oint dx_\mu A_\mu^a T^a \right) \right\rangle. \quad (3)$$

The Feynman diagrams corresponding to this expectation value build up the exponential of the static potential. As a result, in computing the static potential $V^{(-2,j)}$ at order j , iterations of lower order terms in the potential, $V^{(-2,n)}$, $n < j$, are subtracted. At three loops Appelquist, Dine and Muzinich [3] have shown that infrared divergences are encountered in $V^{(-2,4)}(R)$ which are not canceled by simply subtracting iterations of the lower order potentials. Thus, using the definition in Eq. (3) at higher orders in perturbation theory, or generalizing this approach to subleading terms in the v expansion, becomes cumbersome as the set of subtractions become more complicated, and perturbative subtractions are insufficient to render the potential in Eq. (3) well-defined.

A convenient framework for investigating the expansion in Eq. (1) is the effective field theory for non-relativistic QCD (NRQCD), formulated with a power counting in v [4–16].

In the effective field theory, it is more convenient to define the potential as the Wilson coefficient of a four-quark operator [11]

$$\mathcal{L}_p = - \sum_{\mathbf{p}, \mathbf{p}'} V_{\alpha\beta\lambda\tau}(\mathbf{p}, \mathbf{p}') \mu^{2\epsilon} \left[\psi_{\mathbf{p}'}^\dagger_\alpha(x) \psi_{\mathbf{p}\beta}(x) \chi_{-\mathbf{p}'}^\dagger_\lambda(x) \chi_{-\mathbf{p}\tau}(x) \right]. \quad (4)$$

In Eq. (10), the fields ψ and χ annihilate a quark and an antiquark, respectively. The fields are labelled by a momentum \mathbf{p} , and a greek index for their color and spin. The operator in Eq. (4) is local on the scale $x \sim 1/mv^2$, but non-local on the scale $\mathbf{p} \sim mv$. The potential V is computed as a matching coefficient at the scale $\mu = m$ between QCD and an effective theory for non-relativistic QCD valid below the scale m . The effective theory is constructed to have the same infrared structure as perturbative QCD for the two heavy quark system. Therefore, defining the potential as a matching coefficient provides an infrared safe definition. For instance, Ref. [17] shows how the three-loop matching potential V is infrared safe, despite the divergence in the QCD potential of Appelquist, Dine and Muzinich [3].

Although several different formulations of the effective theory for non-relativistic QCD are currently in use [5–16, 18–20], certain universal features have emerged. The on-shell degrees of freedom in the effective theory include quarks with energy $E \sim mv^2$ and momentum $p \sim mv$, soft gluons with $E \sim p \sim mv$, and ultrasoft gluons with $E \sim p \sim mv^2$. The soft and ultrasoft modes are distinct, for instance a consistent power counting in v demands that the ultrasoft gluon interactions are multipole expanded [6, 9], while soft gluon interactions are not. The soft gluons are essential to correctly reproduce the beta function in the effective theory [14], and run between the scales m and mv . Other massless on-shell fields, such as light quarks, will have ultrasoft and soft components too. There are also important off-shell field components, such as the exchange of gluons with $E \sim mv^2$ and $p \sim mv$ that build up the potential. Soft heavy quarks with $E \sim p \sim mv$ are also off-shell relative to the heavy quark states of interest. These off-shell field components can be integrated out of the Lagrangian in the effective theory. Doing this leaves a Lagrangian that is non-local at the scale mv , but local at mv^2 . This procedure, which treats the potential components as four quark operators, was first seriously investigated in Ref. [11], and the resulting effective theory is referred to as pNRQCD. In Ref. [11] it was proposed that the matching onto effective theories should take place in two stages: at $\mu = m$ one matches QCD onto NRQCD as originally defined in Ref. [5], and then matches NRQCD onto pNRQCD at the scale $\mu = mv$.

The matching of four-quark operators at m was considered in Ref. [12], following the proposal in Ref. [8] that the matching procedure should be similar to that in HQET. How-

ever, in general this procedure seems to be slightly problematic [16]. First note that it is necessary to include the kinetic term for the potential quarks immediately below the scale m . For instance, this is necessary to reproduce the threshold value of the two-loop anomalous dimension for the heavy quark production current [21] in the effective theory [16]. With the kinetic energy term included at leading order, the consistency of the v power counting forces us to have both ultrasoft and soft modes *right below* m (along with the multipole expansion etc.). If we note that the kinetic energy term is necessary to correctly reproduce the Coulombic infrared divergences in the effective theory, then it might seem obvious that it must be included in order to have the correct infrared structure. At one-loop, matching exactly at threshold in dimensional regularization seemed to provide a method of avoiding this [12], but this procedure fails at two-loops.

Since we must include the kinetic energy term for all $\mu < m$ it seems quite natural to immediately consider matching at $\mu = m$ onto an effective theory where the off-shell potential gluons and soft quarks have been integrated out. Such a formulation was proposed in Ref. [16] and will be considered in this paper. It will be referred to as vNRQCD. In this theory it is more appropriate to consider the running from m to the scales mv and mv^2 in a single step. This is accomplished by using the velocity renormalization group [16]. Once the vNRQCD effective theory has been run down to the low scale the soft degrees of freedom have served their purpose and may be integrated out. In this final effective theory no additional running needs to be considered.

In this paper we compute the one-loop matching for the $Q\bar{Q}$ and QQ potentials between QCD and vNRQCD up to corrections of order v^2 . Our results are compared to the matching calculation of Pineda and Soto [12] for the four-quark operators and to the threshold expansion [13]. The main difference between the non-relativistic theories in Refs. [16] and [11,12,19] is the way in which large logarithms of v are summed in the effective theory. There is also some difference in the matching corrections; some contributions in vNRQCD that arise at the scale $\mu = m$ are instead computed at $\mu = mv$ in pNRQCD. We will discuss the differences between the two approaches in the text of the paper.

The full QCD calculation of the $Q\bar{Q}$ scattering to order $\alpha_s^2 v^0$ in the non-relativistic expansion has been done before [22,23]. In calculating the potentials, Ref. [22] performs an additional expansion, assuming

$$\frac{(\mathbf{p}' + \mathbf{p})^2}{(\mathbf{p}' - \mathbf{p})^2} \ll 1. \quad (5)$$

In the usual v power counting, \mathbf{p} and \mathbf{p}' are both of order v , so the ratio in Eq. (5) is of order unity, and cannot be treated as small. For this reason, in section II we redo the

QCD calculation keeping the full dependence on this ratio for both the color singlet and octet channels. For the order v^0 spin-independent potential, terms proportional to $(\mathbf{p} + \mathbf{p}')^2$ which were dropped in previous calculations [22,23] are necessary to match infrared divergences between the full and effective theories.

In section III we discuss the order v^0 potential of the form

$$\frac{(\mathbf{p}'^2 - \mathbf{p}^2)^2}{m^2(\mathbf{p}' - \mathbf{p})^4}. \quad (6)$$

For free quark states this potential vanishes on-shell by energy conservation, $\mathbf{p}'^2 = \mathbf{p}^2$, and need not be included in the potential if one uses on-shell matching [24]. The potential in Eq. (6) gives a non-zero contribution in loops or in matrix elements with external Coulomb states, and is often included in the quark potential. For instance, the usual Breit Hamiltonian includes a potential of the form in Eq. (6). A potential that is only non-zero off-shell can be gauge dependent, and including the potential of Eq. (6) induces gauge dependence in the coefficients of on-shell potentials. Using an off-shell potential gives correct results if all calculations are performed in the same gauge. We will use an on-shell basis for the potential where the term in Eq. (6) does not occur. The matching coefficients for the on-shell potential are gauge independent, since scattering amplitudes are measurable quantities. The difference between the on-shell matching potential and the Breit Hamiltonian is compensated for by a corresponding change in the $1/|\mathbf{p}' - \mathbf{p}|$ potential, as discussed in more detail in section III (see also Refs. [25–29]).

In section IV we extend all of our results for the quark-antiquark potential to the quark-quark potential and in section V we give the QED limit of our results. Section VI gives our conclusions.

II. MATCHING THE POTENTIAL TO $\mathcal{O}(v^2)$

The vNRQCD effective Lagrangian has the form

$$\mathcal{L} = \mathcal{L}_u + \mathcal{L}_s + \mathcal{L}_p. \quad (7)$$

The ultrasoft Lagrangian \mathcal{L}_u involves the fields $\psi_{\mathbf{p}}$ which annihilate a quark, $\chi_{\mathbf{p}}$ which annihilate an antiquark, and A^μ which annihilate and create ultrasoft gluons. The potential Lagrangian \mathcal{L}_p contains operators with four or more quark fields including the quark-antiquark potential. Finally the soft Lagrangian \mathcal{L}_s contains all terms that involve soft fields which have energy and momenta of order mv . Heavy quarks with soft energy and momenta are

off-shell and are therefore integrated out, so they do not appear explicitly in \mathcal{L}_s . The terms we need in the ultrasoft Lagrangian are

$$\begin{aligned}\mathcal{L}_u = & -\frac{1}{4}F^{\mu\nu}F_{\mu\nu} + \sum_{\mathbf{p}} \psi_{\mathbf{p}}^\dagger \left\{ iD^0 - \frac{(\mathbf{p} - i\mathbf{D})^2}{2m} + \frac{\mathbf{p}^4}{8m^3} \right\} \psi_{\mathbf{p}} \\ & + \chi_{\mathbf{p}}^\dagger \left\{ iD^0 - \frac{(\mathbf{p} - i\mathbf{D})^2}{2m} + \frac{\mathbf{p}^4}{8m^3} \right\} \chi_{\mathbf{p}}.\end{aligned}\quad (8)$$

The covariant derivative on $\psi_{\mathbf{p}}$ and $\chi_{\mathbf{p}}$ contain the color matrices T^A and \bar{T}^A for the $\mathbf{3}$ and $\bar{\mathbf{3}}$ representations, respectively. Here D^μ involves only the ultrasoft gluon fields: $D^\mu = \partial^\mu + ig\mu_U^\epsilon A^\mu = (D^0, -\mathbf{D})$, so $D^0 = \partial^0 + ig\mu_U^\epsilon A^0$, $\mathbf{D} = \nabla - ig\mu_U^\epsilon \mathbf{A}$. The factors of the ultrasoft scale parameter μ_U^ϵ are included to make $g = g(\mu_U)$ dimensionless in $d = 4 - 2\epsilon$ dimensions. The ultrasoft gluon field A^μ is order v^2 and has dimension $1 - \epsilon$, so $A^\mu \sim (mv^2)^{1-\epsilon}$. Consistency of the v power counting for the covariant derivative in d dimensions then requires $\mu_U = m\nu^2$ where $\nu \sim v$. This reproduces the dependence of μ_U on the subtraction velocity ν given in Ref. [16]. The terms we need in the soft Lagrangian are

$$\begin{aligned}\mathcal{L}_s = & \sum_q \left\{ \left| q^\mu A_q^\nu - q^\nu A_q^\mu \right|^2 + \bar{\varphi}_q \not{D} \varphi_q + \bar{c}_q q^2 c_q \right\} \\ & - g^2 \mu_S^{2\epsilon} \sum_{\mathbf{p}, \mathbf{p}', q, q'} \left\{ \frac{1}{2} \psi_{\mathbf{p}'}^\dagger [A_{q'}^\mu, A_q^\nu] U_{\mu\nu}^{(\sigma)} \psi_{\mathbf{p}} + \frac{1}{2} \psi_{\mathbf{p}'}^\dagger \{A_{q'}^\mu, A_q^\nu\} W_{\mu\nu}^{(\sigma)} \psi_{\mathbf{p}} \right. \\ & \left. + \psi_{\mathbf{p}'}^\dagger [\bar{c}_{q'}, c_q] Y^{(\sigma)} \psi_{\mathbf{p}} + (\psi_{\mathbf{p}'}^\dagger T^B Z_\mu^{(\sigma)} \psi_{\mathbf{p}}) (\bar{\varphi}_{q'} \gamma^\mu T^B \varphi_q) \right\} + (\psi \rightarrow \chi, T \rightarrow \bar{T}),\end{aligned}\quad (9)$$

where A_q , c_q , and φ_q are soft gluons, ghosts, and massless quarks. The functions U , W , Y , and Z are given in Appendix A. After integrating out the soft quarks the Lagrangian \mathcal{L}_s is no longer manifestly gauge invariant with respect to gauge transformations at the scale mv . Therefore, determining the dependence of the soft scale parameter μ_S on ν may seem more difficult than the ultrasoft case. However, prior to integrating out the soft quarks the combination $g\mu_S^\epsilon A_q$ is from a covariant derivative, and $A_q \sim (mv)^{1-\epsilon}$, yielding $\mu_S \sim m\nu$ in agreement with Ref. [16]. In Eq. (9), $g = g(\mu_S)$. In general it is important to realize that the v scaling of μ_U and μ_S are different. If the matching calculation is performed at the scale¹ m , then for this computation $\mu = \mu_S = \mu_U = m$ and $\nu = 1$ (where the usual QCD scale parameter is denoted by μ). Therefore, for the matching at m it is not essential to distinguish between μ_S and μ_U .

¹It is not necessary to match exactly at m . If the matching scale is $\mu = \mu_h \sim m$, then one still sets $\mu_U = \mu_S = \mu_h$ and $\nu = 1$, and factors of $\ln(\mu_h/m)$ appear in the matching coefficients. For convenience we choose $\mu_h = m$ in this paper.

The potential interaction relevant for our calculation is

$$\mathcal{L}_p = - \sum_{\mathbf{p}, \mathbf{p}'} V_{\alpha\beta\lambda\tau}(\mathbf{p}, \mathbf{p}') \mu_S^{2\epsilon} \psi_{\mathbf{p}'\alpha}^\dagger \psi_{\mathbf{p}\beta} \chi_{-\mathbf{p}'}^\dagger \chi_{-\mathbf{p}}. \quad (10)$$

The factor of $\mu_S^{2\epsilon}$ is included so that in $d = 4 - 2\epsilon$ dimensions the potential V has dimension -2 . $\alpha, \beta, \lambda, \tau$ denote color and spin indices. We will use the basis in which the potential is written as a linear combination of $1 \otimes 1$ and $T^a \otimes \bar{T}^a$ in color space. One can convert to the color singlet and octet potential using the linear transformation

$$\begin{bmatrix} V_{\text{singlet}} \\ V_{\text{octet}} \end{bmatrix} = \begin{bmatrix} 1 & -C_F \\ 1 & \frac{1}{2}C_A - C_F \end{bmatrix} \begin{bmatrix} V_{1\otimes 1} \\ V_{T\otimes \bar{T}} \end{bmatrix}, \quad (11)$$

where $C_F = (N_c^2 - 1)/(2N_c)$ and $C_A = N_c$. We will also need the invariants $C_1 = (N_c^2 - 1)/(4N_c^2)$ and $C_d = N_c - 4/N_c$. These arise in the identities

$$\begin{aligned} T^A T^B \otimes \bar{T}^A \bar{T}^B &= -\frac{1}{4}(C_A + C_d)T^A \otimes \bar{T}^A + C_1 1 \otimes 1, \\ T^A T^B \otimes \bar{T}^B \bar{T}^A &= \frac{1}{4}(C_A - C_d)T^A \otimes \bar{T}^A + C_1 1 \otimes 1. \end{aligned} \quad (12)$$

Written as a matrix, the order v^{-2} Coulomb potential is

$$V^{(-2)} = (T^A \otimes \bar{T}^A) \frac{\mathcal{V}_c^{(T)}}{\mathbf{k}^2} + (1 \otimes 1) \frac{\mathcal{V}_c^{(1)}}{\mathbf{k}^2}, \quad (13)$$

where $\mathbf{k} = \mathbf{p}' - \mathbf{p}$, and the coefficients $\mathcal{V}_c^{(T)}$ and $\mathcal{V}_c^{(1)}$ have an expansion in α_s .

The order v^0 potential includes

$$\begin{aligned} V^{(0)} &= (T^A \otimes \bar{T}^A) \left[\frac{\mathcal{V}_2^{(T)}}{m^2} + \frac{\mathcal{V}_r^{(T)}(\mathbf{p}^2 + \mathbf{p}'^2)}{2m^2 \mathbf{k}^2} + \frac{\mathcal{V}_s^{(T)}}{m^2} \mathbf{S}^2 + \frac{\mathcal{V}_\Lambda^{(T)}}{m^2} \Lambda(\mathbf{p}', \mathbf{p}) + \frac{\mathcal{V}_t^{(T)}}{m^2} \mathbf{T}(\mathbf{k}) \right] \\ &+ (1 \otimes 1) \left[\frac{\mathcal{V}_2^{(1)}}{m^2} + \frac{\mathcal{V}_s^{(1)}}{m^2} \mathbf{S}^2 \right], \end{aligned} \quad (14)$$

where

$$\mathbf{S} = \frac{\boldsymbol{\sigma}_1 + \boldsymbol{\sigma}_2}{2}, \quad \Lambda(\mathbf{p}', \mathbf{p}) = -i \frac{\mathbf{S} \cdot (\mathbf{p}' \times \mathbf{p})}{\mathbf{k}^2}, \quad \mathbf{T}(\mathbf{k}) = \boldsymbol{\sigma}_1 \cdot \boldsymbol{\sigma}_2 - \frac{3\mathbf{k} \cdot \boldsymbol{\sigma}_1 \mathbf{k} \cdot \boldsymbol{\sigma}_2}{\mathbf{k}^2}, \quad (15)$$

and $\boldsymbol{\sigma}_1/2$ and $\boldsymbol{\sigma}_2/2$ are the spin-operators on the quark and anti-quark. Note that on-shell $\mathbf{p}'^2 = \mathbf{p}^2$, but we have written $\mathbf{p}^2 + \mathbf{p}'^2$ in Eq. (14) so that the Lagrangian \mathcal{L}_p is hermitian. The tree level diagram in Fig. 1a generates terms of $\mathcal{O}(v^{2k}\alpha_s)$, $k \geq -1$, in the QCD potential. Matching at $\mu = m$, $\nu = 1$ gives

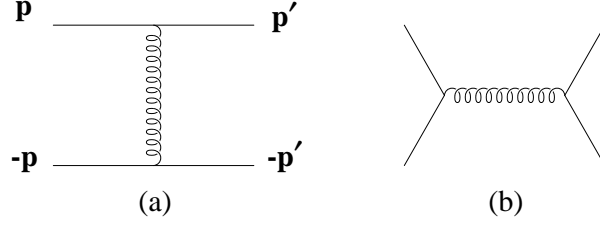


FIG. 1. QCD diagrams for tree level matching.

$$\begin{aligned}
\mathcal{V}_c^{(T)} &= 4\pi\alpha_s(m), & \mathcal{V}_c^{(1)} &= 0, & \mathcal{V}_r^{(T)} &= 4\pi\alpha_s(m), \\
\mathcal{V}_s^{(T)} &= -\frac{4\pi\alpha_s(m)}{3}, & \mathcal{V}_\Lambda^{(T)} &= -6\pi\alpha_s(m), & \mathcal{V}_t^{(T)} &= -\frac{\pi\alpha_s(m)}{3}, \\
\mathcal{V}_s^{(1)} &= 0, & \mathcal{V}_2^{(T)} &= 0, & \mathcal{V}_2^{(1)} &= 0.
\end{aligned} \tag{16}$$

The annihilation diagram in Fig. 1b generates terms of order $\alpha_s v^{2k}$, $k \geq 0$ in the potential. Using Fierz identities and charge conjugation, these operators can be transformed into the basis in Eq. (14) and give additional contributions to the matching. Only $\mathcal{V}_s^{(T,1)}$ receive non-zero annihilation contributions at tree level:

$$\mathcal{V}_{s,a}^{(T)} = \frac{1}{N_c} \pi \alpha_s(m), \quad \mathcal{V}_{s,a}^{(1)} = \frac{(N_c^2 - 1)}{2N_c^2} \pi \alpha_s(m). \tag{17}$$

The complete tree level matching is given by adding the terms in Eqs. (16) and (17). We have found it convenient to distinguish the annihilation contributions by including an additional subscript a on the coefficients they generate. The leading-log values of the order v^0 potentials in Eq. (14) were calculated in Refs. [30,20], but are not needed here. Nonzero values for $\mathcal{V}_2^{(T,1)}$ are generated in the renormalization group flow below the scale m [20], as well as by the one-loop matching as we will see below.

At one-loop the matching onto QCD gives order $1/v$ terms of the form

$$V^{(-1)} = \frac{\pi^2}{m|\mathbf{k}|} \left[\mathcal{V}_k^{(T)} (T^A \otimes \bar{T}^A) + \mathcal{V}_k^{(1)} (1 \otimes 1) \right], \tag{18}$$

where the coefficients $\mathcal{V}_k^{(T,1)}$ are dimensionless. In $d = 4 - 2\epsilon$ dimensions the one-loop matching produces a potential with the dependence $\mu^{2\epsilon}/|\mathbf{k}|^{1+2\epsilon}$. We have chosen to define $V^{(-1)}$ by taking the $d \rightarrow 4$ limit, which differs from the definition of this operator used in Ref. [31].

A. The QCD Calculation

To perform the potential matching calculation, we consider the on-shell $Q\bar{Q}$ scattering amplitude in QCD and in vNRQCD to order $\alpha_s^2 v^0$. We will use Feynman gauge, regulate

infrared divergences with a finite gluon mass² λ , and renormalize ultraviolet divergences with dimensional regularization and the $\overline{\text{MS}}$ scheme. Since the calculation is performed on-shell the resulting matching coefficients will be gauge independent.

We begin by considering the QCD diagrams. The most complicated diagram is the QCD box diagram [32,33] which includes contributions of order $1/v^3$, $1/v^2$, $1/v$ and v^0 , as well as higher order terms which we do not need in this paper.

$$\begin{aligned}
\text{Box Diagram} &= \frac{i\alpha_s^2}{k^2} (T^A T^B \otimes \bar{T}^A \bar{T}^B) \left[\frac{2im\pi}{p} \ln\left(\frac{k^2}{\lambda^2}\right) - 4 \ln\left(\frac{k^2}{\lambda^2}\right) \right. \\
&+ \frac{\pi^2 k}{mp(2p+k)} \left\{ 6p^2 + \frac{5pk}{2} + \frac{k^2}{4} - 3k^2 \Lambda - \left(pk + \frac{5k^2}{6}\right) \mathbf{S}^2 - \frac{k^2 \mathbf{T}}{12} - \frac{k \mathbf{R}}{4(2p+k)} \right\} \\
&+ \frac{6i\pi k^2 \Lambda}{mp(4p^2 - k^2)} \left\{ k^2 \ln\left(\frac{2p}{\lambda}\right) - 4p^2 \ln\left(\frac{k}{\lambda}\right) \right\} \\
&+ \frac{i\pi k^2 \mathbf{S}^2}{3mp(4p^2 - k^2)} \left\{ k^2 - 4p^2 + (5k^2 - 12p^2) \ln\left(\frac{2p}{\lambda}\right) - (4p^2 + k^2) \ln\left(\frac{k}{\lambda}\right) \right\} \\
&+ \frac{i\pi k^2 \mathbf{T}}{6mp(4p^2 - k^2)} \left\{ 4p^2 - k^2 + k^2 \ln\left(\frac{2p}{\lambda}\right) + (-8p^2 + k^2) \ln\left(\frac{k}{\lambda}\right) \right\} \\
&- \frac{i\pi k^2 \mathbf{R}}{2mp(4p^2 - k^2)^2} \left\{ k^2 - 4p^2 + (4p^2 + k^2) \ln\left(\frac{2p}{k}\right) \right\} \\
&+ \frac{i\pi}{2mp(4p^2 - k^2)} \left\{ 4p^2 k^2 - k^4 - k^2(4p^2 + k^2) \ln\left(\frac{2p}{\lambda}\right) \right. \\
&+ (80p^4 - 16p^2 k^2 + k^4) \ln\left(\frac{k}{\lambda}\right) \left. \right\} - \frac{6k^2}{m^2} + \frac{8k^2 \mathbf{S}^2}{3m^2} - \frac{k^2 \mathbf{T}}{3m^2} \\
&+ \ln\left(\frac{\lambda}{k}\right) \left\{ \frac{56p^2}{3m^2} - \frac{12k^2 \Lambda}{m^2} - \frac{8k^2 \mathbf{S}^2}{3m^2} - \frac{2k^2 \mathbf{T}}{3m^2} \right\} + \ln\left(\frac{k}{m}\right) \left\{ \frac{4k^2}{m^2} - \frac{2k^2 \mathbf{S}^2}{m^2} \right\} \Big],
\end{aligned} \tag{19}$$

where $k = |\mathbf{k}|$, $p = |\mathbf{p}| = |\mathbf{p}'|$ and

$$\mathbf{R} = (\mathbf{p} + \mathbf{p}') \cdot \boldsymbol{\sigma}_1 (\mathbf{p} + \mathbf{p}') \cdot \boldsymbol{\sigma}_2. \tag{20}$$

The real part of the order $1/v$ amplitude agrees with Ref. [22] in the limit $p \rightarrow k/2$. We have kept the full p dependence since taking this limit is not justified by the power counting. We have also kept imaginary terms generated by the cut amplitude to emphasize how these terms are correctly reproduced in the effective theory. The real part of the spin dependent order v^0 amplitude agree with the result in Ref. [34]. The real part of the spin independent order v^0 amplitude agrees with Ref. [23], except for the order $v^0 \ln(k)$ and $\ln(\lambda)$ dependence.

²Using a finite gluon mass is dangerous in the presence of diagrams with the non-abelian gluon vertices. All such diagrams we require here are IR finite in Feynman gauge.

The difference is due to the condition $|\mathbf{p}' + \mathbf{p}| \ll k$ which was imposed in Refs. [22,23], but which violates the v power counting. (For the crossed box given below in Eq. (21a), the order $v^0 \ln(\lambda)$ and $\ln(k)$ also differs from Ref. [23].) The remaining direct scattering diagrams are less complicated since they have no cuts:

$$\begin{aligned}
\text{Diagram (Crossed Box)} &= \frac{i\alpha_s^2}{k^2} (T^A T^B \otimes \bar{T}^B \bar{T}^A) \left[4 \ln \left(\frac{k^2}{\lambda^2} \right) - \frac{\pi^2 k}{m} \right. \\
&\quad + \ln \left(\frac{\lambda}{k} \right) \left\{ \frac{8k^2}{3m^2} - \frac{56p^2}{3m^2} + \frac{12k^2 \Lambda}{m^2} + \frac{8k^2 \mathbf{S}^2}{3m^2} + \frac{2k^2 \mathbf{T}}{3m^2} \right\} \\
&\quad \left. + \ln \left(\frac{k}{m} \right) \left\{ -\frac{6k^2}{m^2} + \frac{2k^2 \mathbf{S}^2}{m^2} \right\} + \frac{2k^2}{m^2} - \frac{2k^2 \mathbf{S}^2}{3m^2} + \frac{k^2 \mathbf{T}}{3m^2} \right], \quad (21a)
\end{aligned}$$

$$\begin{aligned}
\text{Diagram (Triangle)} &+ \text{Diagram (Triangle)} = -\frac{i\alpha_s^2}{k^2} C_A (T^A \otimes \bar{T}^A) \left[3 \ln \left(\frac{\mu^2}{m^2} \right) + 4 + \frac{\pi^2 k}{2m} \right. \\
&\quad + \ln \left(\frac{k}{m} \right) \left\{ \frac{4k^2}{m^2} - \frac{4k^2 \mathbf{S}^2}{3m^2} - \frac{k^2 \mathbf{T}}{3m^2} - \frac{4k^2 \Lambda}{m^2} \right\} \\
&\quad + \ln \left(\frac{\mu}{m} \right) \left\{ \frac{6p^2}{m^2} - \frac{9k^2 \Lambda}{m^2} - \frac{2k^2 \mathbf{S}^2}{m^2} - \frac{k^2 \mathbf{T}}{2m^2} \right\} \\
&\quad \left. + \frac{4p^2}{m^2} - \frac{8k^2 \Lambda}{m^2} - \frac{2k^2 \mathbf{S}^2}{m^2} - \frac{k^2 \mathbf{T}}{2m^2} \right], \quad (21b)
\end{aligned}$$

$$\begin{aligned}
\text{Diagram (Box)} &+ \text{Diagram (Box)} = -\frac{i\alpha_s^2}{k^2} (2C_F - C_A) (T^A \otimes \bar{T}^A) \left[\left\{ 2 \ln \left(\frac{\lambda^2}{m^2} \right) + \ln \left(\frac{\mu^2}{m^2} \right) + 4 \right\} M^0 \right. \\
&\quad \left. + \frac{k^2}{m^2} - \frac{2k^2 \mathbf{S}^2}{3m^2} - \frac{k^2 \mathbf{T}}{6m^2} - \frac{2k^2 \Lambda}{m^2} + \frac{4k^2}{3m^2} \ln \left(\frac{\lambda}{m} \right) \right], \quad (21c)
\end{aligned}$$

$$\text{Diagram (Box)} + \text{perms} = \frac{i\alpha_s^2}{k^2} 2C_F (T^A \otimes \bar{T}^A) \left\{ 2 \ln \left(\frac{\lambda^2}{m^2} \right) + \ln \left(\frac{\mu^2}{m^2} \right) + 4 \right\} M^0, \quad (21d)$$

$$\text{Diagram (Box)} + \text{Diagram (Box)} = -\frac{i\alpha_s^2}{k^2} C_A (T^A \otimes \bar{T}^A) \left\{ \frac{5}{3} \ln \left(\frac{\mu^2}{k^2} \right) + \frac{31}{9} \right\} M^0, \quad (21e)$$

and the light quark loops for n_f flavors gives:

$$\text{Diagram (Box)} = \frac{i\alpha_s^2}{k^2} n_f T_F (T^A \otimes \bar{T}^A) \left\{ \frac{4}{3} \ln \left(\frac{\mu^2}{k^2} \right) + \frac{20}{9} \right\} M^0, \quad (21f)$$

while the heavy quark fermion loop gives:

$$\begin{array}{c} \text{---} \text{---} \\ | \\ \text{---} \text{---} \end{array} = \frac{i\alpha_s^2}{k^2} T_F(T^A \otimes \bar{T}^A) \left\{ \frac{4}{3} \ln\left(\frac{\mu^2}{m^2}\right) M^0 - \frac{4k^2}{15m^2} \right\}. \quad (21g)$$

In Eq. (21) the matrix element

$$M^0 = 1 + \frac{p^2}{m^2} - \frac{k^2 \mathbf{S}^2}{3m^2} - \frac{3k^2 \Lambda}{2m^2} - \frac{k^2 \mathbf{T}}{12m^2}. \quad (22)$$

Note that we disagree with Ref. [23] on the order v^0 spin independent part of Eq. (21b). Ref. [23] has an additional non-logarithmic $1/m^2$ term. The difference arises because we find a different value for the order k^2 term in the non-Abelian F_1 form-factor. Eqs. (21c) through (21g) agree with Ref. [23].

The diagrams in Eq. (19) and (21) have contributions from several different scales. In particular, in the language of the threshold expansion [13], the hard regime gives $\ln(\mu/m)$'s, the soft regime gives $\ln(\mu/k)$'s, and the ultrasoft regime gives $\ln(\mu/\lambda)$'s. There are also $i \ln(\lambda/p)$ and $i \ln(\lambda/k)$ terms from the Coulomb divergence in the potential regime. In addition to logarithms, all regimes can give constant factors. In the effective theory, terms from the hard regime are absorbed into matching coefficients such as the four-quark potential operators and the remaining terms correspond to graphs involving modes in the effective theory. These graphs are discussed in more detail below.

Next consider the one-loop annihilation diagrams in QCD. Since the intermediate gluons are hard we expect these graphs to include a factor of $1/m^2$, thus giving hard order v^0 contributions to the potential. However, the graph in Eq. (23c) also has terms enhanced by a factor of m/p , which are order $1/v$ contributions.

$$\begin{array}{c} \text{---} \text{---} \\ | \\ \text{---} \text{---} \end{array} + \begin{array}{c} \text{---} \text{---} \\ | \\ \text{---} \text{---} \end{array} = -\frac{i\alpha_s^2}{m^2} \left[\left\{ \left(\frac{C_1}{N_c} + \frac{C_d(N_c^2-1)}{8N_c^2} \right) (1 \otimes 1) + \left(\frac{C_d}{4N_c} - 2C_1 \right) (T^A \otimes \bar{T}^A) \right\} \right. \\ \times (\mathbf{S}^2 - 2)(i\pi + 2 - 2 \ln 2) - C_A \left\{ \frac{(N_c^2-1)}{2N_c^2} (1 \otimes 1) + \frac{1}{N_c} (T^A \otimes \bar{T}^A) \right\} \\ \left. \times \mathbf{S}^2 \left\{ \frac{i\pi}{12} + \frac{1}{6} - \frac{\ln 2}{6} - \ln\left(\frac{\lambda}{m}\right) \right\} \right], \quad (23a)$$

$$\begin{array}{c} \text{---} \text{---} \\ | \\ \text{---} \text{---} \end{array} + \begin{array}{c} \text{---} \text{---} \\ | \\ \text{---} \text{---} \end{array} = -\frac{i\alpha_s^2}{m^2} C_A \left\{ (T^A \otimes \bar{T}^A) \frac{1}{N_c} + (1 \otimes 1) \frac{(N_c^2-1)}{2N_c} \right\} \\ \times \mathbf{S}^2 \left\{ \frac{3}{2} \ln\left(\frac{\mu}{m}\right) + \frac{4}{3} + \frac{2 \ln 2}{3} - \frac{i\pi}{3} \right\}, \quad (23b)$$

$$\begin{array}{c} \text{---} \text{---} \\ | \\ \text{---} \text{---} \end{array} + \begin{array}{c} \text{---} \text{---} \\ | \\ \text{---} \text{---} \end{array} = -\frac{i\alpha_s^2}{4m^2} (2C_F - C_A) \left\{ (T^A \otimes \bar{T}^A) \frac{1}{N_c} + (1 \otimes 1) \frac{(N_c^2-1)}{2N_c} \right\} \\ \times \mathbf{S}^2 \left\{ \frac{\pi^2 m}{p} + \frac{2i\pi m}{p} \ln\left(\frac{2p}{\lambda}\right) - 4 + 2 \ln\left(\frac{\mu}{m}\right) + 4 \ln\left(\frac{\lambda}{m}\right) \right\}, \quad (23c)$$

$$\begin{aligned}
\text{Diagram} + \text{perms} &= \frac{i\alpha_s^2}{m^2} C_F \left\{ (T^A \otimes \bar{T}^A) \frac{1}{N_c} + (1 \otimes 1) \frac{(N_c^2 - 1)}{2N_c} \right\} \\
&\times \mathbf{S}^2 \left\{ \ln \left(\frac{\lambda^2}{m^2} \right) + \ln \left(\frac{\mu}{m} \right) + 2 \right\}, \tag{23d}
\end{aligned}$$

$$\begin{aligned}
\text{Diagram} + \text{Diagram} &= -\frac{i\alpha_s^2}{m^2} \frac{5C_A}{12} \left\{ (T^A \otimes \bar{T}^A) \frac{1}{N_c} + (1 \otimes 1) \frac{(N_c^2 - 1)}{2N_c} \right\} \\
&\times \mathbf{S}^2 \left\{ \ln \left(\frac{\mu^2}{m^2} \right) - 2 \ln 2 + \frac{31}{15} + i\pi \right\}, \tag{23e}
\end{aligned}$$

and the light quark loop for n_f flavors gives:

$$\begin{aligned}
\text{Diagram} &= \frac{i\alpha_s^2}{m^2} \frac{n_f T_F}{3} \left\{ (T^A \otimes \bar{T}^A) \frac{1}{N_c} + (1 \otimes 1) \frac{(N_c^2 - 1)}{2N_c} \right\} \\
&\times \mathbf{S}^2 \left\{ \ln \left(\frac{\mu^2}{m^2} \right) - 2 \ln 2 + \frac{5}{3} + i\pi \right\}, \tag{23f}
\end{aligned}$$

while the heavy quark loop gives:

$$\begin{aligned}
\text{Diagram} &= \frac{i\alpha_s^2}{m^2} \frac{T_F}{3} \left\{ (T^A \otimes \bar{T}^A) \frac{1}{N_c} + (1 \otimes 1) \frac{(N_c^2 - 1)}{2N_c} \right\} \\
&\times \mathbf{S}^2 \left\{ \ln \left(\frac{\mu^2}{m^2} \right) + \frac{8}{3} \right\}. \tag{23g}
\end{aligned}$$

In the limit $p \rightarrow k/2$, the results in Eq. (23) agree with Ref. [22], except for Fig. (23c) and differences that can be accounted for by the fact that we are using $\overline{\text{MS}}$ rather than an on-shell subtraction scheme. For Fig. (23c), Ref. [22] has a π^2/k term which for us is $-\pi^2/(2p)$. This sign for the π^2/p term is in agreement with Ref. [35]. The imaginary parts of these one-loop annihilation amplitudes also agree with Ref. [5]. Note that in Eqs. (19), (21), and (23), $\alpha_s = \alpha_s(\mu)$.

B. The Effective Theory Calculation

The effective theory contains potential, soft and ultrasoft loops. We have organized the terms by their order in the velocity expansion. The order in v can be determined using the v power counting formula³ in Eq. (40) of Ref. [16]. A loop graph with two insertions of the Coulomb potential contributes to a $1/v^3$ potential, and with an insertion of one Coulomb and one $V^{(0)}$ potential contributes to a $1/v$ potential. A soft loop with two vertices of order

³Here the power of v is given for the amputated diagram, so unlike Eq. (40) in Ref. [16] the factors of v associated with external lines are not included.

σ and σ' contributes to the $v^{\sigma+\sigma'-2}$ potential. Graphs involving the exchange of an ultrasoft gluon begin to contribute to the potential at order v^0 , etc.

1. Order $1/v^3$

In the effective theory taking two insertions of the tree level Coulomb potential in a loop gives the only diagram that is order α_s^2/v^3 :

$$\text{Diagram} = i \frac{[\mathcal{V}_c^{(T)}]^2}{16\pi^2} (T^A T^B \otimes \bar{T}^A \bar{T}^B) \frac{2im\pi}{k^2 p} \ln\left(\frac{k^2}{\lambda^2}\right). \quad (24)$$

Taking $\mu = m$ and $\nu = 1$ and using the tree level value of $V_c^{(T)}$, this graph exactly reproduces the order α_s^2/v^3 ‘‘Coulomb singularity’’ term in the QCD box diagram in Eq. (19). Thus, there is no matching correction at this order.

2. Order $1/v^2$

At order α_s^2/v^2 in the effective theory, the only non-zero diagram involves the exchange of soft gluons, ghosts and quarks:

$$\text{Diagram} = \frac{i\alpha_s^2(\mu_S)}{k^2} (T^A \otimes \bar{T}^A) \left[\frac{4T_F n_f - 11C_A}{3} \left\{ \frac{1}{\hat{\epsilon}} + \ln\left(\frac{\mu_S^2}{k^2}\right) \right\} + \frac{20T_F n_f - 31C_A}{9} \right], \quad (25)$$

where $1/\hat{\epsilon} = 1/\epsilon - \gamma + \ln(4\pi)$ is the combination subtracted in $\overline{\text{MS}}$. The divergence in this graph is responsible for the one-loop running of $\mathcal{V}_c^{(T)}$. At one-loop, to order v^0 the effective theory counterterms (and running of the potential) were computed in Ref. [20] and from now on the $1/\hat{\epsilon}$ dependence will be dropped. The sum of order α_s^2/v^2 terms from the QCD diagrams in Eqs. (19) and (21) is

$$\frac{i\alpha_s^2(\mu)}{k^2} (T^A \otimes \bar{T}^A) \left[\frac{4T_F}{3} \ln\left(\frac{\mu^2}{m^2}\right) + \frac{4T_F n_f - 11C_A}{3} \ln\left(\frac{\mu^2}{k^2}\right) + \frac{20T_F n_f - 31C_A}{9} \right]. \quad (26)$$

At the scale $\mu = \mu_S = m$ the $\overline{\text{MS}}$ values of Eq. (25) and Eq. (26) are identical, so there is no one-loop matching correction to \mathcal{V}_c . The difference in $\ln(\mu)$ ’s in Eqs. (26) and (25) is the change in β -function from $n_f + 1$ to n_f flavors. We would expect a new contribution to \mathcal{V}_c only if the QCD graphs have a contribution from the hard regime where energy and momenta are order m . In Eqs. (21b), (21c), and (21d), the factors of $-3\ln(m^2) + 4$ are from the hard regime, but they sum to zero. For the $\ln(m)$ terms this is a consequence of the

Ward identity derived in Ref. [3]. The constant factor $(20T_F n_f - 31C_A)/9$ vanishes in the matching condition at m , and is carried to scales below m by the soft modes.

Note that if at the scale $\nu = v_k \sim k/m$ we integrate out the soft modes, then the Coulomb potential for the theory below this scale, $\bar{\mathcal{V}}_c$, will obtain an additional contribution from this second stage of matching: $\bar{\mathcal{V}}_c^{(T)}(v_k) = \mathcal{V}_c^{(T)}(v_k) - (20T_F n_f - 31C_A)\alpha_s^2(mv_k)/9$. In this expression $\mathcal{V}_c^{(T)}(v_k)$ is the value of $\mathcal{V}_c^{(T)}$ obtained from running this coefficient from $\nu = 1$ to $\nu = v_k$ using its two-loop anomalous dimension. This reproduces the constant factor that is typically associated with the Coulomb potential at next-to-leading order (see for instance, Ref. [1]). Similarly, one can obtain the additional terms from the matching contributions for the v^0 potentials at mv from the value of the soft loops given in Eq. (31).

3. Order $1/v$

The possible order α_s^2/v diagrams with soft gluons vanish explicitly, so the only order α_s^2/v diagrams in the effective theory involve two iterations of the potential. There are two diagrams with insertions of $\mathcal{V}_c^{(T)}$:

$$\begin{array}{c} \mathcal{V}_c \\ \diagup \quad \diagdown \\ \bullet \quad \times \quad \bullet \\ \diagdown \quad \diagup \\ \mathcal{V}_c \end{array} + \Delta E \begin{array}{c} \mathcal{V}_c \\ \diagup \quad \diagdown \\ \bullet \quad \bullet \\ \diagdown \quad \diagup \\ \mathcal{V}_c \end{array} = \frac{i[\mathcal{V}_c^{(T)}]^2}{4m} T^A T^B \otimes \bar{T}^A \bar{T}^B (I_F + 2p^2 I_0), \quad (27)$$

where the integrals I_0 and I_F are given in Appendix B. The dependence on $\mathcal{V}_c^{(1)}$ is not needed since tree level matching gives $\mathcal{V}_c^{(1)} = 0$. In the first diagram in Eq. (27), the cross denotes an insertion of the \mathbf{p}^4/m^3 operator from Eq. (8). The second diagram is nominally order α_s^2/v^3 ; however it depends on the heavy quark energy $E = \mathbf{p}^2/(2m) - \mathbf{p}^4/(8m^3) + \dots$. When the energy is expanded in terms of momenta, the graph includes a contribution of order α_s^2/v which we indicate by the pre-factor ΔE in Eq. (27). Each of the diagrams in Eq. (27) has an IR divergence that is not regulated by λ , but the IR divergence in the sum of the integrands for the two diagrams is regulated.

Additional α_s^2/v diagrams are generated by including one insertion of the Coulomb potential and one order v^0 potential:

$$\begin{array}{c} \mathcal{V}_c \\ \diagup \quad \diagdown \\ \bullet \quad \square \\ \diagdown \quad \diagup \\ \mathcal{V}_r \end{array} + \begin{array}{c} \mathcal{V}_r \\ \diagup \quad \diagdown \\ \square \quad \bullet \\ \diagdown \quad \diagup \\ \mathcal{V}_c \end{array} = \frac{i\mathcal{V}_c^{(T)}\mathcal{V}_r^{(T)}}{m} T^A T^B \otimes \bar{T}^A \bar{T}^B (I_F + 2p^2 I_0), \quad (28a)$$

$$\begin{array}{c} \mathcal{V}_c \\ \diagup \quad \diagdown \\ \bullet \quad \square \\ \diagdown \quad \diagup \\ \mathcal{V}_s \end{array} + \begin{array}{c} \mathcal{V}_s \\ \diagup \quad \diagdown \\ \square \quad \bullet \\ \diagdown \quad \diagup \\ \mathcal{V}_c \end{array} = \frac{i\mathcal{V}_c^{(T)}\mathcal{V}_s^{(T)}}{m} T^A T^B \otimes \bar{T}^A \bar{T}^B (2I_P \mathbf{S}^2), \quad (28b)$$

$$\begin{array}{c} \mathcal{V}_c \quad \mathcal{V}_\Lambda \\ \diagdown \quad \diagup \\ \bullet \quad \square \\ \diagup \quad \diagdown \end{array} + \begin{array}{c} \mathcal{V}_\Lambda \quad \mathcal{V}_c \\ \diagdown \quad \diagup \\ \square \quad \bullet \\ \diagup \quad \diagdown \end{array} = \frac{i\mathcal{V}_c^{(T)}\mathcal{V}_\Lambda^{(T)}}{m} T^A T^B \otimes \bar{T}^A \bar{T}^B \left(2k^2 \Lambda(\mathbf{p}', \mathbf{p}) I_A \right), \quad (28c)$$

$$\begin{array}{c} \mathcal{V}_c \quad \mathcal{V}_t \\ \diagdown \quad \diagup \\ \bullet \quad \square \\ \diagup \quad \diagdown \end{array} + \begin{array}{c} \mathcal{V}_t \quad \mathcal{V}_c \\ \diagdown \quad \diagup \\ \square \quad \bullet \\ \diagup \quad \diagdown \end{array} = \frac{-i\mathcal{V}_c^{(T)}\mathcal{V}_t^{(T)}}{2m} T^A T^B \otimes \bar{T}^A \bar{T}^B \left[\mathbf{k} \cdot \sigma_1 \mathbf{k} \cdot \sigma_2 (12I_C + 3I_0) \right. \\ \left. - 4\sigma_1 \cdot \sigma_2 (I_P - 3I_B) + \mathbf{R} (12I_D - 12I_A + 3I_0) \right], \quad (28d)$$

$$\begin{array}{c} \mathcal{V}_c \quad \mathcal{V}_{s,a} \\ \diagdown \quad \diagup \\ \bullet \quad \square \\ \diagup \quad \diagdown \end{array} + \begin{array}{c} \mathcal{V}_{s,a} \quad \mathcal{V}_c \\ \diagdown \quad \diagup \\ \square \quad \bullet \\ \diagup \quad \diagdown \end{array} = \frac{i\mathcal{V}_c^{(T)}\mathcal{V}_{s,a}^{(T)}}{m} T^A T^B \otimes \bar{T}^A \bar{T}^B \left(\mathbf{S}^2 2I_P \right) \\ + \frac{i\mathcal{V}_c^{(T)}\mathcal{V}_{s,a}^{(1)}}{m} T^A \otimes \bar{T}^A \left(\mathbf{S}^2 2I_P \right). \quad (28e)$$

The last two diagrams involve insertions of terms in the potential generated by the tree level annihilation diagram. In Eqs. (27) and (28) the dependence on $1 \otimes 1$ potentials whose coefficients vanish at tree level are not shown. Thus, both the $1 \otimes 1$ and $T \otimes \bar{T}$ contributions are only shown in Eq. (28e). The new integrals I_P , I_A , I_B , I_C , and I_D that appear in Eq. (28) are given in Appendix B, and \mathbf{R} is defined in Eq. (20).

The infrared divergences in the $1/v$ amplitude are due to the Coulomb singularity. The divergences in the full theory are reproduced by the potential loops in Eqs. (27) and (28). The imaginary terms in the amplitude from the QCD box graph exactly agree with those in the effective theory, and do not contribute in the matching coefficients, as expected. Subtracting the effective theory graphs in Eqs. (27) and (28) from the order α_s^2/v terms in Eq. (19), (21)a,b and (23)c gives the matching result for the $V^{(-1)}$ potential at $\mu = m$, $\nu = 1$:

$$\mathcal{V}_k^{(T)} = \alpha_s^2(m) \left(\frac{7C_A}{8} - \frac{C_d}{8} \right), \quad \mathcal{V}_k^{(1)} = \alpha_s^2(m) \frac{C_1}{2}. \quad (29)$$

For the color singlet channel this gives the matching coefficient $\mathcal{V}_k^{(s)} = \alpha_s^2(m) (C_F^2/2 - C_F C_A)$ in agreement with Ref. [23]. Note that the real part of the $1/v$ amplitudes in the full and effective theory have a complicated dependence on p and k , but the momentum dependence of the matching for the direct potentials in Eq. (29) is only of the form $1/|\mathbf{k}|$. For the annihilation graphs the $1/p$ terms cancel between the full and effective theories. There would have been a $1/p$ matching coefficient for the annihilation graphs if the results of Ref. [22] had been used for the full theory graph.

The matching coefficients in Eq. (29) correspond to a contribution to the $1/v$ potential at the scale $\mu = m$, which does not come from the hard part of any graph. This is in apparent

contradiction with the threshold expansion. It also appears to disagree with Refs. [19] and [31], where the $1/|\mathbf{k}|$ four-quark potential operator is said to only arise at the scale mv . However, in Refs. [19] and [31] a formulation of NRQCD is being used in which off-shell potential field components have not been integrated out for scales $mv < \mu < m$, but instead are considered to be dynamical fields in the Lagrangian (see Refs. [7,10]). In the full theory the $1/|\mathbf{k}|$ terms come from three types of graphs, shown in Eq. (19) and Eqs. (21a,b). At the scale m there are now effective theory graphs analogous to those in Eq. (21b) but with two A^0 potential gluons and one \mathbf{A}^i potential gluon, which reproduce the $1/|\mathbf{k}|$ term. For the box and crossed box in Feynman gauge the $1/|\mathbf{k}|$ terms are reproduced by contributions that can be associated with the potential momentum regime. Thus, in Refs. [19] and [31] the $1/|\mathbf{k}|$ potential in Eq. (29) effectively exists at the scale m . In our approach off-shell potential gluons and soft quarks are integrated out, so the matching for the $1/|\mathbf{k}|$ potential is not simply given by the hard part of the QCD diagrams.

4. Order v^0

For the order $\alpha_s^2 v^0$ matching we will consider the direct and annihilation diagrams separately. The sum of the order $\alpha_s^2 v^0$ terms in the direct scattering QCD diagrams in Eqs. (19) and (21) is

$$\begin{aligned}
& -\frac{i\alpha_s^2(\mu)}{m^2} (1 \otimes 1) C_1 \left[4 - 2\mathbf{S}^2 + 2 \ln\left(\frac{k}{m}\right) - \frac{8}{3} \ln\left(\frac{\lambda}{k}\right) \right] \\
& -\frac{i\alpha_s^2(\mu)}{m^2} (T^A \otimes \bar{T}^A) \left[\frac{p^2}{k^2} \left\{ \frac{31C_A}{9} + \frac{16C_A}{3} \ln\left(\frac{\lambda}{\mu}\right) + \frac{38C_A}{3} \ln\left(\frac{\mu}{k}\right) \right\} \right. \\
& \quad + \left\{ 2C_F - 3C_A - C_d + \left(\frac{8C_F}{3} + \frac{2C_d}{3} - 2C_A \right) \ln\left(\frac{\lambda}{\mu}\right) \right. \\
& \quad + \left(\frac{7C_d}{6} - \frac{43C_A}{6} \right) \ln\left(\frac{\mu}{k}\right) + \left(\frac{8C_F}{3} + \frac{31C_A}{6} - \frac{C_d}{2} \right) \ln\left(\frac{\mu}{m}\right) \Big\} \\
& \quad + \Lambda \left\{ -\frac{31C_A}{6} - 4C_F - 7C_A \ln\left(\frac{\mu}{k}\right) - 4C_A \ln\left(\frac{\mu}{m}\right) \right\} \\
& \quad + \mathbf{S}^2 \left\{ \frac{C_d}{2} - \frac{17C_A}{54} - \frac{4C_F}{3} - \frac{C_A}{9} \ln\left(\frac{\mu}{k}\right) - \frac{7C_A}{3} \ln\left(\frac{\mu}{m}\right) \right\} \\
& \quad + \mathbf{T} \left\{ -\frac{49C_A}{108} - \frac{C_F}{3} - \frac{5C_A}{18} \ln\left(\frac{\mu}{k}\right) - \frac{C_A}{3} \ln\left(\frac{\mu}{m}\right) \right\} \\
& \quad - n_f T_F \left\{ \frac{4}{3} \ln\left(\frac{\mu^2}{k^2}\right) + \frac{20}{9} \right\} \left\{ \frac{p^2}{k^2} - \frac{\mathbf{S}^2}{3} - \frac{3\Lambda}{2} - \frac{\mathbf{T}}{12} \right\} \\
& \quad \left. - \frac{4T_F}{3} \ln\left(\frac{\mu^2}{m^2}\right) \left\{ \frac{p^2}{k^2} - \frac{\mathbf{S}^2}{3} - \frac{3\Lambda}{2} - \frac{\mathbf{T}}{12} \right\} + \frac{4T_F}{15} \right].
\end{aligned} \tag{30}$$

The effective theory contribution from order $\alpha_s^2 v^0$ diagrams with soft gluons, ghosts or quarks is:

$$\begin{aligned}
\text{Diagram} &= \frac{i\alpha_s^2(\mu_S)}{m^2} (1 \otimes 1) \left[\frac{14C_1}{3} \ln\left(\frac{\mu_S}{k}\right) - \frac{C_1}{3} \right] \\
&+ \frac{i\alpha_s^2(\mu_S)}{m^2} (T^A \otimes \bar{T}^A) \left[C_A \ln\left(\frac{\mu_S}{k}\right) \left\{ \frac{43}{6} - \frac{38p^2}{3k^2} + 7\Lambda + \frac{\mathbf{S}^2}{9} + \frac{5\mathbf{T}}{18} \right\} \right. \\
&\quad \left. - \frac{7C_d}{6} \ln\left(\frac{\mu_S}{k}\right) + \frac{C_d}{12} + \frac{7C_A}{3} - \frac{31C_A p^2}{9k^2} + \frac{7C_A \Lambda}{6} - \frac{14C_A \mathbf{S}^2}{27} + \frac{13C_A \mathbf{T}}{108} \right. \\
&\quad \left. + n_f T_F \left\{ \frac{4}{3} \ln\left(\frac{\mu_S^2}{k^2}\right) + \frac{20}{9} \right\} \left\{ \frac{p^2}{k^2} - \frac{\mathbf{S}^2}{3} - \frac{3\Lambda}{2} - \frac{\mathbf{T}}{12} \right\} \right].
\end{aligned} \tag{31}$$

There are also non-zero order $\alpha_s^2 v^0$ diagrams with an ultrasoft gluon and one insertion of the Coulomb potential. These diagrams were calculated in Ref. [20]:

$$\begin{aligned}
\text{Diagram} + \dots &= \frac{8i}{3m^2} \alpha_s(\mu_S) \alpha_s(\mu_U) \ln\left(\frac{\mu_U}{\lambda}\right) \left[-C_1(1 \otimes 1) \right. \\
&\quad \left. + (T \otimes \bar{T}) \left\{ C_F + \frac{C_d}{4} - \frac{3C_A}{4} + \frac{2p^2 C_A}{k^2} \right\} \right].
\end{aligned} \tag{32}$$

In Eq. (32) the ellipses denote all possible diagrams that are generated by attaching the ultrasoft gluon to two fermion legs. Subtracting the sum of Eq. (31) and (32) from Eq. (30) and setting $\mu = \mu_S = \mu_U = m$ gives the one-loop matching contribution for the order v^0 direct potentials. At order v^0 we find that all the infrared divergences in QCD are matched by infrared divergences from the effective theory graphs with ultrasoft gluons. All $\ln(k)$'s in the full theory are matched by $\ln(k)$'s in Eq. (31). The contributions to the matching coefficients at one-loop are:

$$\begin{aligned}
\mathcal{V}_r^{(T)} &= 0, & \mathcal{V}_r^{(1)} &= 0, \\
\mathcal{V}_\Lambda^{(T)} &= -4(C_F + C_A) \alpha_s^2(m), & \mathcal{V}_\Lambda^{(1)} &= 0, \\
\mathcal{V}_s^{(T)} &= \left(\frac{1}{2}C_d - \frac{5}{6}C_A - \frac{4}{3}C_F \right) \alpha_s^2(m), & \mathcal{V}_s^{(1)} &= -2C_1 \alpha_s^2(m), \\
\mathcal{V}_t^{(T)} &= -\frac{1}{3}(C_F + C_A) \alpha_s^2(m), & \mathcal{V}_t^{(1)} &= 0, \\
\mathcal{V}_2^{(T)} &= \left(2C_F - \frac{11}{12}C_d - \frac{2}{3}C_A + \frac{4}{15}T_F \right) \alpha_s^2(m), & \mathcal{V}_2^{(1)} &= \frac{11}{3} C_1 \alpha_s^2(m).
\end{aligned} \tag{33}$$

The total order $\alpha_s^2 v^0$ matching coefficients are given by adding the tree level values in Eq. (16) to the results in Eq. (33), and are summarized in Table I at the end of the paper.

Next consider the matching of the order $\alpha_s^2 v^0$ annihilation contributions. Since there are no corresponding diagrams in the effective theory, the sum of the $\alpha_s^2 v^0$ terms in Eq. (23)

directly give the matching coefficients. This sum is infrared finite. Matching at $\mu = m$, $\nu = 1$ we find that the one-loop annihilation contributions to the potential coefficients are:

$$\begin{aligned}
\mathcal{V}_{s,a}^{(T)} &= \left(\frac{C_d}{4N_c} - 2C_1 \right) (i\pi + 2 - 2\ln 2) \alpha_s^2(m) \\
&\quad + \frac{1}{N_c} \left\{ \frac{109C_A}{36} - 4C_F + \frac{n_f T_F}{3} \left(2\ln 2 - \frac{5}{3} - i\pi \right) - \frac{8T_F}{9} \right\} \alpha_s^2(m), \\
\mathcal{V}_{s,a}^{(1)} &= \left\{ \frac{C_1}{N_c} + \frac{C_d(N_c^2 - 1)}{8N_c^2} \right\} (i\pi + 2 - 2\ln 2) \alpha_s^2(m) \\
&\quad + \frac{(N_c^2 - 1)}{2N_c^2} \left\{ \frac{109C_A}{36} - 4C_F + \frac{n_f T_F}{3} \left(2\ln 2 - \frac{5}{3} - i\pi \right) - \frac{8T_F}{9} \right\} \alpha_s^2(m), \\
\mathcal{V}_{2,a}^{(T)} &= -2 \left(\frac{C_d}{4N_c} - 2C_1 \right) (i\pi + 2 - 2\ln 2) \alpha_s^2(m), \\
\mathcal{V}_{2,a}^{(1)} &= -2 \left\{ \frac{C_1}{N_c} + \frac{C_d(N_c^2 - 1)}{8N_c^2} \right\} (i\pi + 2 - 2\ln 2) \alpha_s^2(m). \tag{34}
\end{aligned}$$

The imaginary terms in these potentials contribute to the cross section for annihilation of a color octet heavy quark and anti-quark into light hadrons, and agree with the results of Ref. [5]. The total annihilation contribution to the order $\alpha_s^2 v^0$ matching coefficients are given by adding the tree level results in Eq. (17) to the results in Eq. (34), and are summarized in Table I.

If a different matching scale, μ_h , had been used then the coefficients in Eqs. (33) and (34) would also depend on $\ln(\mu_h/m)$. Since the prediction for observables is independent of μ_h the most convenient choice, $\mu_h = m$, has been adopted.

In the threshold expansion, the full QCD diagram is the sum of hard, soft, ultrasoft and potential graphs. The soft, ultrasoft and potential graphs are the graphs in the effective theory up to renormalization effects such as the dependence on the scales μ_S and μ_U . The matching conditions in Eq. (33) and (34) can also be computed from the hard part of the full theory graphs, and we have verified that this gives the same result as in Eqs. (33) and (34). The matching onto four-quark operators was first considered by Pineda and Soto in the context of pNRQCD [12]. In their approach, the hard parts of the vertex correction and wavefunction renormalization are included in matching coefficients in the single heavy quark sector of the Lagrangian. The direct matching for four-quark operators is given by the hard part of the box and crossed-box. The hard part of our box and crossed-box agree with Ref. [12], except for the finite part of the $\sigma_1 \cdot \sigma_2$ terms, which causes our $\mathcal{V}_2^{(T)}$ and $\mathcal{V}_s^{(T)}$ to disagree with theirs. This is related to the treatment of epsilon tensors and the non-relativistic reduction of matrix elements of spin operators in d dimensions. We have chosen to take the lowest order term in the matrix element of $\gamma^{[\alpha} \gamma^\sigma \gamma^{\beta]} \otimes \gamma_{[\alpha} \gamma_\tau \gamma_{\beta]}$ to be

$\epsilon^{\alpha\beta\sigma k} \epsilon_{\alpha\beta\tau k'} \sigma_1^k \sigma_2^{k'}$, and have used the 't Hooft-Veltmann scheme for the epsilon tensors so that $\epsilon_{\mu\nu\alpha\beta}$ and ϵ^{ijk} are only non-zero when the indices are in four and three dimensions respectively. This convention was used in both the soft loop integrals as well as when cross checking our result by computing the hard part of the box diagrams using the threshold expansion. This scheme dependence is related to the issue of evanescent operators [36–38]. The annihilation results in Eq. (34) agree completely with Ref. [12].

Note that in a leading-log expansion the two-loop anomalous dimension is needed at the same time as the one-loop matching results. In the color-singlet channel the $1/v^2$ two-loop anomalous dimensions is known [1,2], since the running of the Coulomb potential is still given by the QCD β -function at this order. The result for the two-loop anomalous dimension for $V^{(-1)}$ will be presented in another publication [39].

III. TERMS IN THE POTENTIAL WHICH VANISH ON-SHELL.

For the scattering $Q(p_1^0, \mathbf{p}) + \bar{Q}(p_2^0, -\mathbf{p}) \rightarrow Q(p_3^0, \mathbf{p}') + \bar{Q}(p_4^0, -\mathbf{p}')$ consider adding

$$\begin{aligned} V^{(0)} = & \left[\mathcal{V}_{\Delta 1}^{(T)} (T^A \otimes \bar{T}^A) + \mathcal{V}_{\Delta 1}^{(1)} (1 \otimes 1) \right] \frac{(p_3^0 - p_1^0)^2}{\mathbf{k}^4} \\ & + \left[\mathcal{V}_{\Delta 2}^{(T)} (T^A \otimes \bar{T}^A) + \mathcal{V}_{\Delta 2}^{(1)} (1 \otimes 1) \right] \frac{(\mathbf{p}'^2 - \mathbf{p}^2)^2}{4m^2 \mathbf{k}^4} \end{aligned} \quad (35)$$

to the potential in Eq. (14). Here $\mathbf{k} = \mathbf{p}' - \mathbf{p}$ and by energy conservation $p_3^0 - p_1^0 = p_2^0 - p_4^0$. On-shell the potentials in Eq. (35) vanish, since $p_1^0 = p_3^0$, $p_4^0 = p_2^0$, and $\mathbf{p}^2 = \mathbf{p}'^2$. However, if we work off-shell, they are valid terms and in fact show up in many calculations that make use of time-ordered perturbation theory.

Matching to the tree level diagrams in Fig. 1 with $p_1^0 \neq p_3^0$ gives a contribution to the potentials in Eq. (35). In Feynman gauge one finds

$$\mathcal{V}_{\Delta 1}^{(T)} = 4\pi\alpha_s(m), \quad \mathcal{V}_{\Delta 1}^{(1)} = 0, \quad \mathcal{V}_{\Delta 2}^{(T)} = 0, \quad \mathcal{V}_{\Delta 2}^{(1)} = 0, \quad (36)$$

while in Coulomb gauge one gets a different answer

$$\mathcal{V}_{\Delta 1}^{(T)} = 0, \quad \mathcal{V}_{\Delta 1}^{(1)} = 0, \quad \mathcal{V}_{\Delta 2}^{(T)} = -4\pi\alpha_s(m), \quad \mathcal{V}_{\Delta 2}^{(1)} = 0. \quad (37)$$

Unlike the on-shell potentials discussed in the previous section, the matching conditions for off-shell potentials are gauge dependent. Using the expressions for the soft vertices in Feynman gauge in Appendix A, the one loop anomalous dimensions are

$$\nu \frac{\partial}{\partial \nu} \mathcal{V}_{\Delta 2}^{(T)} = -2\beta_0 \alpha_s (m\nu)^2, \quad \nu \frac{\partial}{\partial \nu} \mathcal{V}_{\Delta 1}^{(T)} = \nu \frac{\partial}{\partial \nu} \mathcal{V}_{\Delta 1}^{(1)} = \nu \frac{\partial}{\partial \nu} \mathcal{V}_{\Delta 2}^{(1)} = 0. \quad (38)$$

Including the potential in Eq. (35) modifies the matching condition for the $1/|\mathbf{k}|$ potentials and also makes this matching gauge dependent. This is because in the effective theory there are now two new order α_s^2/v diagrams:

$$\begin{array}{c} \mathcal{V}_c \quad \mathcal{V}_\Delta \\ \diagup \quad \diagdown \end{array} \quad \begin{array}{c} \mathcal{V}_\Delta \quad \mathcal{V}_c \\ \diagup \quad \diagdown \end{array} = \frac{i\mathcal{V}_c^{(T)}\mathcal{V}_\Delta^{(T)}}{32mk} T^A T^B \otimes \bar{T}^A \bar{T}^B + \frac{i\mathcal{V}_c^{(T)}\mathcal{V}_\Delta^{(1)}}{32mk} T^A \otimes \bar{T}^A + \dots \quad (39)$$

In Eq. (39) the box labeled by \mathcal{V}_Δ denotes an insertion of both operators in Eq. (35), the ellipses denote operators that vanish by the equations of motion (proportional to $p_1^0 - \mathbf{p}^2/2m$, $p_3^0 - \mathbf{p}'^2/2m$ etc.), and we have defined

$$\mathcal{V}_\Delta^{(T)} = \mathcal{V}_{\Delta 1}^{(T)} + \mathcal{V}_{\Delta 2}^{(T)}, \quad \mathcal{V}_\Delta^{(1)} = \mathcal{V}_{\Delta 1}^{(1)} + \mathcal{V}_{\Delta 2}^{(1)}. \quad (40)$$

In Feynman gauge the matching conditions in Eq. (29) now become

$$\mathcal{V}_{kF}^{(T)} = \alpha_s^2(m) \left(\frac{3C_A}{4} - \frac{C_d}{4} \right), \quad \mathcal{V}_{kF}^{(1)} = \alpha_s^2(m) C_1, \quad (41)$$

while in Coulomb gauge

$$\mathcal{V}_{kC}^{(T)} = C_A \alpha_s^2(m), \quad \mathcal{V}_{kC}^{(1)} = 0. \quad (42)$$

The $1/|\mathbf{k}|$ potential is often referred to as the non-abelian potential. From Eqs. (41) and (42), we see that the $1/|\mathbf{k}|$ potential only vanishes in QED if the potential is taken to include off-shell components and Coulomb gauge is used.

The result in Eq. (39) shows that in the off-shell matching potential one can make the replacements

$$\begin{aligned} V_\Delta^{(T)} &\rightarrow V_\Delta^{(T)} + \zeta^{(T)}, \\ V_\Delta^{(1)} &\rightarrow V_\Delta^{(1)} + \zeta^{(1)}, \\ V_k^{(T)} &\rightarrow V_k^{(T)} + \frac{1}{32\pi^2} V_c^{(T)} \left[\zeta^{(1)} - \frac{1}{4} (C_A + C_d) \zeta^{(T)} \right], \\ V_k^{(1)} &\rightarrow V_k^{(1)} + \frac{1}{32\pi^2} V_c^{(T)} C_1 \zeta^{(T)}, \end{aligned} \quad (43)$$

for arbitrary $\zeta^{(T,1)}$. For instance, at the matching scale taking $\zeta^{(1)} = 0$, $\zeta^{(T)} = -8\pi\alpha_s(m)$ effectively transforms the Feynman gauge result in Eqs. (36) and (41) into the Coulomb gauge result in Eqs. (37) and (42). Furthermore, taking $\zeta^{(1)} = 0$ and $\zeta^{(T)} = 4\pi\alpha_s(m)$ transforms the off-shell Coulomb gauge result into the on-shell result in section II. These transformations convert terms in the potential that are order $\alpha_s v^0$ to order α_s^2/v . Similar transformations for the position space color singlet potentials have been pointed out previously in Refs. [25–27].

IV. THE QUARK-QUARK POTENTIAL

The quark-quark potentials in the effective theory can be defined in the same way as the quark-antiquark potentials. The only difference is that the $V^{(T)}$ terms are now the coefficient of the $T^A \otimes T^A$ tensor, rather than the $T^A \otimes \bar{T}^A$ tensor. The computation of the quark-quark potential is almost identical to that of the quark-antiquark potential. The result can be obtained from the quark-antiquark potential by omitting the annihilation terms, and making the substitutions $C_d \rightarrow -C_d$ and $\bar{T}^A \rightarrow T^A$. The change in sign of C_d arises from the identities in Eq. (12). Replacing \bar{T} by T in these equations changes the sign of the C_d terms.

The potential in the symmetric and antisymmetric QQ color channels (the **6** and $\bar{\mathbf{3}}$ for $SU(3)$) are given by

$$\begin{bmatrix} V_{\text{symmetric}} \\ V_{\text{antisymmetric}} \end{bmatrix} = \begin{bmatrix} 1 & \frac{N_c-1}{2N_c} \\ 1 & -\frac{N_c+1}{2N_c} \end{bmatrix} \begin{bmatrix} V_{1\otimes 1} \\ V_{T\otimes T} \end{bmatrix}. \quad (44)$$

The spin-1 QQ combination is spin-symmetric and the spin-0 QQ combination is spin-antisymmetric. For identical fermions in the initial state, for the symmetric spin-color states we must antisymmetrize the potential in the momenta, $V = V(\mathbf{p}, \mathbf{p}') - V(-\mathbf{p}, \mathbf{p}')$, and for the antisymmetric spin-color states we must symmetrize the potential in the momenta, $V = V(\mathbf{p}, \mathbf{p}') + V(-\mathbf{p}, \mathbf{p}')$. This corresponds to including the crossed diagrams in the computation of the potentials.

V. QED

It is straightforward to obtain the QED potential from our results. For oppositely charged particles of charge $\pm Q$, the QED direct potential is given by $Q^2(V_{1\otimes 1} - V_{T\otimes \bar{T}})$, where $V_{1\otimes 1}$ and $V_{T\otimes \bar{T}}$ are given by our QCD results with $C_1 = C_F = T_F = 1$, $C_A = C_d = 0$, and $\alpha_s \rightarrow \alpha$. The on-shell $1/|\mathbf{k}|$ potential does not vanish in this limit. In the results for the annihilation potentials at the scale m in Eqs. (17) and (34), explicit factors of N_c were included in the Fierz transformation, so it is simplest to just separately list the QED limit of these results:

$$\begin{aligned} \mathcal{V}_{s,a}^{(T)} &= -(i\pi + 2 - 2\ln 2) \alpha^2(m) Q^2, \\ \mathcal{V}_{s,a}^{(1)} &= \pi \alpha(m) + \left\{ -\frac{44}{9} + \frac{n_f}{3} \left(2\ln 2 - \frac{5}{3} - i\pi \right) \right\} \alpha^2(m) Q^2, \\ \mathcal{V}_{2,a}^{(T)} &= 2(i\pi + 2 - 2\ln 2) \alpha^2(m) Q^2, \\ \mathcal{V}_{2,a}^{(1)} &= 0. \end{aligned} \quad (45)$$

For e^+e^- we have $n_f = 0$ and the terms in our v^0 potentials agree with Ref. [15].

For identical particles with charge Q , there is only the direct potential contribution, which is given by $Q^2(V_{1\otimes 1} + V_{T\otimes T})$, with $C_1 = C_F = T_F = 1$, $C_A = C_d = 0$, and $\alpha_s \rightarrow \alpha$ as above. As discussed in Section IV, including the crossed diagrams gives a final potential that is symmetric or antisymmetric in the momenta depending on the symmetry of the spin state.

VI. CONCLUSION

We have computed the $Q\bar{Q}$ and QQ scattering amplitudes in QCD to order v^2 , and compared our results with previous calculations. We have also computed the scattering graphs in vNRQCD, and computed the matching condition at $\mu = m$ between the two theories. The matching potential was computed using on-shell matching, omitting terms which vanish by the equations of motion. The result was compared with approaches that include terms in the potential that vanish on-shell. The one-loop matching coefficients are summarized in Table I, and can be combined with the two-loop running to give the potential at next to leading log order. The computation of the heavy quark production current at next to leading logarithmic order uses these results and will be discussed in a subsequent publication [39].

We would like to thank A. Hoang and J. Soto for discussions. This work was supported in part by the Department of Energy under grant DOE-FG03-97ER40546.

TABLE I. Matching coefficients for the quark-antiquark potential at $\mu = m$, $\nu = 1$. The tree-level contributions are the order α_s terms, and the one-loop corrections are the order α_s^2 terms. The values are for the on-shell potential, so all off-shell potentials such as the V_Δ potentials in Eq. (35) are set to zero. Contributions to the matching from annihilation diagrams are given separately and are denoted by an extra subscript a .

$\mathcal{V}_c^{(T)}$	$4\pi\alpha_s(m)$
$\mathcal{V}_c^{(1)}$	0
$\mathcal{V}_k^{(T)}$	$\alpha_s^2(m)\left(\frac{7}{8}C_A - \frac{1}{8}C_d\right)$
$\mathcal{V}_k^{(1)}$	$\alpha_s^2(m)\frac{1}{2}C_1$
$\mathcal{V}_r^{(T)}$	$4\pi\alpha_s(m)$
$\mathcal{V}_r^{(1)}$	0
$\mathcal{V}_\Lambda^{(T)}$	$-6\pi\alpha_s(m) - 4(C_F + C_A)\alpha_s^2(m)$
$\mathcal{V}_\Lambda^{(1)}$	0
$\mathcal{V}_s^{(T)}$	$-\frac{4}{3}\pi\alpha_s(m) + \left(\frac{1}{2}C_d - \frac{5}{6}C_A - \frac{4}{3}C_F\right)\alpha_s^2(m)$
$\mathcal{V}_s^{(1)}$	$-2C_1\alpha_s^2(m)$
$\mathcal{V}_t^{(T)}$	$-\frac{1}{3}\pi\alpha_s(m) - \frac{1}{3}(C_F + C_A)\alpha_s^2(m)$
$\mathcal{V}_t^{(1)}$	0
$\mathcal{V}_2^{(T)}$	$\left(2C_F - \frac{11}{12}C_d - \frac{2}{3}C_A + \frac{4}{15}T_F\right)\alpha_s^2(m)$
$\mathcal{V}_2^{(1)}$	$\frac{11}{3}C_1\alpha_s^2(m)$
$\mathcal{V}_{s,a}^{(T)}$	$\frac{1}{N_c}\pi\alpha_s(m) + \left(\frac{1}{4N_c}C_d - 2C_1\right)(i\pi + 2 - 2\ln 2)\alpha_s^2(m)$ $+ \frac{1}{N_c}\left\{\frac{109}{36}C_A - 4C_F + \frac{n_f T_F}{3}\left(2\ln 2 - \frac{5}{3} - i\pi\right) - \frac{8T_F}{9}\right\}\alpha_s^2(m)$
$\mathcal{V}_{s,a}^{(1)}$	$\frac{(N_c^2-1)}{2N_c^2}\pi\alpha_s(m) + \left\{\frac{1}{N_c}C_1 + \frac{(N_c^2-1)}{8N_c^2}C_d\right\}(i\pi + 2 - 2\ln 2)\alpha_s^2(m)$ $+ \frac{(N_c^2-1)}{2N_c^2}\left\{\frac{109}{36}C_A - 4C_F + \frac{n_f T_F}{3}\left(2\ln 2 - \frac{5}{3} - i\pi\right) - \frac{8T_F}{9}\right\}\alpha_s^2(m)$
$\mathcal{V}_{2,a}^{(T)}$	$-2\left(\frac{1}{4N_c}C_d - 2C_1\right)(i\pi + 2 - 2\ln 2)\alpha_s^2(m)$
$\mathcal{V}_{2,a}^{(1)}$	$-2\left\{\frac{1}{N_c}C_1 + \frac{(N_c^2-1)}{8N_c^2}C_d\right\}(i\pi + 2 - 2\ln 2)\alpha_s^2(m)$

APPENDIX A: COEFFICIENTS FOR THE SOFT LAGRANGIAN

The coefficient functions for the soft Lagrangian in Eq. (9) in Feynman gauge are:

$$\begin{aligned}
U_{00}^{(0)} &= \frac{1}{q^0}, \quad U_{0i}^{(0)} = -\frac{(2\mathbf{p}' - 2\mathbf{p} - \mathbf{q})^i}{(\mathbf{p}' - \mathbf{p})^2}, \quad U_{i0}^{(0)} = -\frac{(\mathbf{p} - \mathbf{p}' - \mathbf{q})^i}{(\mathbf{p}' - \mathbf{p})^2}, \quad U_{ij}^{(0)} = \frac{-2q^0\delta^{ij}}{(\mathbf{p}' - \mathbf{p})^2}, \\
U_{00}^{(1)} &= \frac{(\mathbf{p}' + \mathbf{p}) \cdot \mathbf{q}}{2m(q^0)^2} - \frac{(\mathbf{p}' + \mathbf{p}) \cdot \mathbf{q}}{m(\mathbf{p}' - \mathbf{p})^2} - \frac{ic_F \boldsymbol{\sigma} \cdot [\mathbf{q} \times (\mathbf{p} - \mathbf{p}')] }{m(\mathbf{p}' - \mathbf{p})^2} + \frac{(\mathbf{p}'^2 - \mathbf{p}^2)}{2m(\mathbf{p}' - \mathbf{p})^2}, \quad (\text{A1}) \\
U_{0i}^{(1)} &= -\frac{(\mathbf{p} + \mathbf{p}')^i}{2mq^0} + \frac{ic_F(\mathbf{q} \times \boldsymbol{\sigma})^i}{2mq^0} + \frac{q^0(\mathbf{p} + \mathbf{p}')^i}{2m(\mathbf{p}' - \mathbf{p})^2} + \frac{ic_F q^0[(\mathbf{p} - \mathbf{p}') \times \boldsymbol{\sigma}]^i}{2m(\mathbf{p}' - \mathbf{p})^2}, \\
U_{i0}^{(1)} &= -\frac{(\mathbf{p} + \mathbf{p}')^i}{2mq^0} - \frac{ic_F[(\mathbf{p} - \mathbf{p}' + \mathbf{q}) \times \boldsymbol{\sigma}]^i}{2mq^0} + \frac{q^0(\mathbf{p} + \mathbf{p}')^i}{2m(\mathbf{p}' - \mathbf{p})^2} + \frac{ic_F q^0[(\mathbf{p} - \mathbf{p}') \times \boldsymbol{\sigma}]^i}{2m(\mathbf{p}' - \mathbf{p})^2}, \\
U_{ij}^{(1)} &= \frac{ic_F \epsilon^{ijk} \boldsymbol{\sigma}^k}{2m} + [2\delta^{ij} \mathbf{q}^m + \delta^{im}(2\mathbf{p}' - 2\mathbf{p} - \mathbf{q})^j + \delta^{jm}(\mathbf{p} - \mathbf{p}' - \mathbf{q})^i] \\
&\quad \times \left[\frac{(\mathbf{p} + \mathbf{p}')^m + ic_F \epsilon^{mkl}(\mathbf{p} - \mathbf{p}')^k \boldsymbol{\sigma}^l}{2m(\mathbf{p}' - \mathbf{p})^2} \right], \\
U_{00}^{(2)} &= -\frac{c_D(\mathbf{p}' - \mathbf{p})^2}{8m^2q^0} + \frac{c_S i\boldsymbol{\sigma} \cdot (\mathbf{p}' \times \mathbf{p})}{4m^2q^0} + \frac{(\mathbf{p} \cdot \mathbf{q})^2 + (\mathbf{p}' \cdot \mathbf{q})^2}{2m^2(q^0)^3} + \frac{(2 - c_D)(\mathbf{p} - \mathbf{p}') \cdot \mathbf{q}}{4m^2q^0} \\
&\quad + \frac{(1 - c_D)\mathbf{q}^2}{4m^2q^0}, \\
U_{0i}^{(2)} &= -\frac{[\mathbf{p} \cdot \mathbf{q}(2\mathbf{p} + \mathbf{q})^i + \mathbf{p}' \cdot \mathbf{q}(2\mathbf{p}' - \mathbf{q})^i]}{4m^2(q^0)^2} + \frac{ic_F[\mathbf{q} \times \boldsymbol{\sigma}]^i(\mathbf{p} + \mathbf{p}') \cdot \mathbf{q}}{4m^2(q^0)^2} \\
&\quad + \frac{(c_D - 1)(\mathbf{p} - \mathbf{p}' + \mathbf{q})^i}{4m^2} + \frac{(2\mathbf{p}' - 2\mathbf{p} - \mathbf{q})^i}{4m^2} \left[\frac{c_D}{2} - \frac{c_S i\boldsymbol{\sigma} \cdot (\mathbf{p}' \times \mathbf{p})}{(\mathbf{p}' - \mathbf{p})^2} \right] \\
&\quad + \frac{(\mathbf{p}'^2 - \mathbf{p}^2)}{4m^2(\mathbf{p}' - \mathbf{p})^2} \left[(\mathbf{p} + \mathbf{p}')^i + c_F i\boldsymbol{\sigma} \cdot (\mathbf{p}' \times \mathbf{p}) \right] - \frac{(2\mathbf{p}' - 2\mathbf{p} - \mathbf{q})^i(\mathbf{p}'^2 - \mathbf{p}^2)^2}{4m^2(\mathbf{p}' - \mathbf{p})^4}, \\
U_{i0}^{(2)} &= -\frac{[\mathbf{p} \cdot \mathbf{q}(\mathbf{p} + \mathbf{p}' + \mathbf{q})^i + \mathbf{p}' \cdot \mathbf{q}(\mathbf{p} + \mathbf{p}' - \mathbf{q})^i]}{4m^2(q^0)^2} - \frac{ic_F[(\mathbf{p} - \mathbf{p}' + \mathbf{q}) \times \boldsymbol{\sigma}]^i(\mathbf{p} + \mathbf{p}') \cdot \mathbf{q}}{4m^2(q^0)^2} \\
&\quad + \frac{(c_D - 1)\mathbf{q}^i}{4m^2} + \frac{(\mathbf{p} - \mathbf{p}' - \mathbf{q})^i}{4m^2} \left[\frac{c_D}{2} - \frac{c_S i\boldsymbol{\sigma} \cdot (\mathbf{p}' \times \mathbf{p})}{(\mathbf{p}' - \mathbf{p})^2} \right] \\
&\quad - \frac{(\mathbf{p}'^2 - \mathbf{p}^2)}{2m^2(\mathbf{p}' - \mathbf{p})^2} \left[(\mathbf{p} + \mathbf{p}')^i + c_F i\boldsymbol{\sigma} \cdot (\mathbf{p}' \times \mathbf{p}) \right] - \frac{(\mathbf{p} - \mathbf{p}' - \mathbf{q})^i(\mathbf{p}'^2 - \mathbf{p}^2)^2}{4m^2(\mathbf{p}' - \mathbf{p})^4}, \\
U_{ij}^{(2)} &= \frac{(\mathbf{p} + \mathbf{p}')^i(\mathbf{p} + \mathbf{p}')^j}{4m^2q^0} + \frac{c_F^2(\mathbf{p} - \mathbf{p}') \cdot \mathbf{q} \delta^{ij}}{4m^2q^0} + \frac{ic_F(\mathbf{p} + \mathbf{p}')^j[(\mathbf{p} - \mathbf{p}') \times \boldsymbol{\sigma}]^i}{4m^2q^0} \\
&\quad - \frac{ic_F \epsilon^{ijk} \mathbf{q}^k \boldsymbol{\sigma} \cdot (\mathbf{p} + \mathbf{p}')}{4m^2q^0} + \frac{ic_F \epsilon^{ijk} \boldsymbol{\sigma}^k(\mathbf{p} + \mathbf{p}') \cdot \mathbf{q}}{4m^2q^0} + \frac{(1 - c_F^2)\mathbf{q}^i(\mathbf{p} - \mathbf{p}' + \mathbf{q})^j}{4m^2q^0}
\end{aligned}$$

$$\begin{aligned}
& + \frac{c_F^2 \mathbf{q}^2 \delta^{ij}}{4m^2 q^0} - \frac{i \delta^{ij} q^0 c_S i \boldsymbol{\sigma} \cdot (\mathbf{p}' \times \mathbf{p})}{2m^2 (\mathbf{p}' - \mathbf{p})^2} - \frac{2q^0 \delta^{ij} (\mathbf{p}'^2 - \mathbf{p}^2)^2}{4m^2 (\mathbf{p}' - \mathbf{p})^4}, \\
W_{\mu\nu}^{(0)} &= 0, \\
W_{00}^{(1)} &= \frac{1}{2m} + \frac{(\mathbf{p} - \mathbf{p}') \cdot \mathbf{q}}{2m(q^0)^2}, \quad W_{0i}^{(1)} = -\frac{(\mathbf{p} - \mathbf{p}' + \mathbf{q})^i}{2mq^0}, \quad W_{i0}^{(1)} = \frac{-\mathbf{q}^i}{2mq^0}, \quad W_{ij}^{(1)} = \frac{\delta^{ij}}{2m}, \\
Y^{(0)} &= \frac{-q^0}{(\mathbf{p}' - \mathbf{p})^2}, \quad Y^{(1)} = \frac{\mathbf{q} \cdot (\mathbf{p} + \mathbf{p}') + i c_F \boldsymbol{\sigma} \cdot [\mathbf{q} \times (\mathbf{p} - \mathbf{p}')]}{2m(\mathbf{p}' - \mathbf{p})^2}, \\
Y^{(2)} &= \frac{c_D q^0}{8m^2} - \frac{c_S i \boldsymbol{\sigma} \cdot (\mathbf{p}' \times \mathbf{p}) q^0}{4m^2 (\mathbf{p}' - \mathbf{p})^2}, \\
Z_0^{(0)} &= \frac{1}{(\mathbf{p}' - \mathbf{p})^2}, \quad Z_i^{(0)} = 0, \quad Z_0^{(1)} = 0, \quad Z_i^{(1)} = \frac{-(\mathbf{p} + \mathbf{p}')^i - i c_F [(\mathbf{p} - \mathbf{p}') \times \boldsymbol{\sigma}]^i}{2m(\mathbf{p}' - \mathbf{p})^2}, \\
Z_0^{(2)} &= -\frac{1}{4m^2} \left[\frac{c_D}{2} - \frac{c_S i \boldsymbol{\sigma} \cdot (\mathbf{p}' \times \mathbf{p})}{(\mathbf{p}' - \mathbf{p})^2} \right], \quad Z_i^{(2)} = 0.
\end{aligned}$$

These expressions differ from those in Ref. [20] by terms proportional to $\mathbf{p}'^2 - \mathbf{p}^2$, and the values in Eq. (A1) are the complete on-shell expressions. The $\mathbf{p}'^2 - \mathbf{p}^2$ terms were not needed in calculating the one-loop running of the on-shell order v^0 potentials in Ref. [20]. In section III, these terms were used to compute the running of the off-shell potential in Eq. (38), and this result depends on the fact that we used the on-shell soft Lagrangian. The coefficients in Eq. (A1) can be written in a manifestly Hermitian form, however we have instead used $\mathbf{q}' = \mathbf{q} + \mathbf{p} - \mathbf{p}'$ and $q'^0 = q^0 + p^0 - p'^0$ to eliminate q' since this form is more convenient for calculations. Reparameterization invariance [40] can be used to eliminate c_S by the relation $c_S = 2c_F - 1$. The running of c_D and c_F are given in Refs. [41].

APPENDIX B: INTEGRALS

The effective theory integrals that appear in Eqs. (27) and (28) are

$$\begin{aligned}
I_0 &= \int d^3 q \frac{1}{[(\mathbf{q} - \mathbf{p})^2 + \lambda^2][(\mathbf{q} - \mathbf{p}')^2 + \lambda^2][\mathbf{q}^2 - \mathbf{p}^2 - i\epsilon]} = \frac{-i}{8\pi|\mathbf{p}|\mathbf{k}^2} \ln \left(\frac{\lambda^2}{\mathbf{k}^2} \right), \\
I_F &= \int d^3 q \frac{1}{(\mathbf{q} - \mathbf{p})^2 (\mathbf{q} - \mathbf{p}')^2} = \frac{1}{8|\mathbf{k}|}, \\
I_P &= \int d^3 q \frac{1}{[(\mathbf{q} - \mathbf{p}')^2 + \lambda^2][\mathbf{q}^2 - \mathbf{p}^2 - i\epsilon]} = \frac{1}{16|\mathbf{p}|} + \frac{i}{8\pi|\mathbf{p}|} \ln \left(\frac{2|\mathbf{p}|}{\lambda} \right),
\end{aligned} \tag{B1}$$

and

$$\int d^3 q \frac{\mathbf{q}^i}{[(\mathbf{q} - \mathbf{p})^2 + \lambda^2][(\mathbf{q} - \mathbf{p}')^2 + \lambda^2][\mathbf{q}^2 - \mathbf{p}^2 - i\epsilon]} = (\mathbf{p}' + \mathbf{p})^i I_A, \tag{B2}$$

$$\int d^3q \frac{\mathbf{q}^i \mathbf{q}^j}{[(\mathbf{q} - \mathbf{p})^2 + \lambda^2][(\mathbf{q} - \mathbf{p}')^2 + \lambda^2][\mathbf{q}^2 - \mathbf{p}^2 - i\epsilon]} = \delta^{ij} I_B + (\mathbf{p}' - \mathbf{p})^i (\mathbf{p}' - \mathbf{p})^j I_C \\ + (\mathbf{p}' + \mathbf{p})^i (\mathbf{p}' + \mathbf{p})^j I_D ,$$

where $\mathbf{k} = \mathbf{p}' - \mathbf{p}$ and

$$I_A = \frac{(2|\mathbf{p}||\mathbf{k}| - \mathbf{k}^2)\pi - 2i\mathbf{k}^2 \ln\left(\frac{2|\mathbf{p}|}{\lambda}\right) - 4i\mathbf{p}^2 \ln\left(\frac{\lambda^2}{\mathbf{k}^2}\right)}{16\pi|\mathbf{p}|\mathbf{k}^2(4\mathbf{p}^2 - \mathbf{k}^2)} , \quad (\text{B3})$$

$$I_B = \frac{(2|\mathbf{p}| - |\mathbf{k}|)\pi + 2i|\mathbf{p}| \ln\left(\frac{4\mathbf{p}^2}{\mathbf{k}^2}\right)}{16\pi(4\mathbf{p}^2 - \mathbf{k}^2)} ,$$

$$I_C = \frac{(2|\mathbf{p}||\mathbf{k}| - \mathbf{k}^2)\pi - 2i(4\mathbf{p}^2 - \mathbf{k}^2) - 2i\mathbf{k}^2 \ln\left(\frac{2|\mathbf{p}|}{\lambda}\right) - 4i\mathbf{p}^2 \ln\left(\frac{\lambda^2}{\mathbf{k}^2}\right)}{32\pi|\mathbf{p}|\mathbf{k}^2(4\mathbf{p}^2 - \mathbf{k}^2)} ,$$

$$I_D = \frac{1}{32\pi|\mathbf{p}|\mathbf{k}^2(4\mathbf{p}^2 - \mathbf{k}^2)^2} \left[(2|\mathbf{p}| - |\mathbf{k}|)^2(4|\mathbf{p}| + |\mathbf{k}|)|\mathbf{k}|\pi + 2i\mathbf{k}^2(4\mathbf{p}^2 - \mathbf{k}^2) \right. \\ \left. - 2i\mathbf{k}^2(12\mathbf{p}^2 - \mathbf{k}^2) \ln\left(\frac{2|\mathbf{p}|}{\lambda}\right) - 4i\mathbf{p}^2(4\mathbf{p}^2 + \mathbf{k}^2) \ln\left(\frac{\lambda^2}{\mathbf{k}^2}\right) \right] .$$

REFERENCES

- [1] M. Peter, Phys. Rev. Lett. **78**, 602 (1997).
- [2] Y. Schröder, Phys. Lett. **B447** 321 (1999).
- [3] T. Appelquist, M. Dine and I. Muzinich, Phys. Lett. **B69**, 231, (1977); T. Appelquist, M. Dine and I. Muzinich, Phys. Rev. **D17**, 2074, (1978).
- [4] W.E. Caswell and G.P. Lepage, Phys. Lett. **167B**, 437 (1986).
- [5] G.T. Bodwin, E. Braaten and G.P. Lepage, Phys. Rev. **D51**, 1125 (1995), Erratum ibid. **D55**, 5853 (1997).
- [6] P. Labelle, Phys. Rev. **D58**, 093013 (1998).
- [7] M. Luke and A.V. Manohar, Phys. Rev. **D55**, 4129 (1997).
- [8] A.V. Manohar, Phys. Rev. **D56**, 230 (1997).
- [9] B. Grinstein and I.Z. Rothstein, Phys. Rev. **D57**, 78 (1998).
- [10] M. Luke and M.J. Savage, Phys. Rev. **D57**, 413 (1998).
- [11] A. Pineda and J. Soto, Nucl. Phys. Proc. Suppl. **64**, 428 (1998);
- [12] A. Pineda and J. Soto, Phys. Rev. **D58**, 114011 (1998).
- [13] M. Beneke and V.A. Smirnov, Nucl. Phys. **B522**, 321 (1998).
- [14] H.W. Griesshammer, Phys. Rev. **D58**, 094027 (1998).
- [15] A. Pineda and J. Soto, Phys. Rev. **D59** 016005 (1999).
- [16] M.E. Luke, A.V. Manohar, and I.Z. Rothstein, hep-ph/9910209.
- [17] N. Brambilla, A. Pineda, J. Soto, and A. Vairo, Phys. Rev. **D60**, 091502 (1999).
- [18] B. A. Kniehl and A. A. Penin, Nucl. Phys. **B563**, 200 (1999); B. A. Kniehl and A. A. Penin, hep-ph/9911414.
- [19] N. Brambilla, A. Pineda, J. Soto and A. Vairo, Phys. Lett. **B470**, 215 (1999); Nucl. Phys. **B566**, 275 (2000).
- [20] A.V. Manohar and I.W. Stewart, hep-ph/9912226.
- [21] For QED see: A.H. Hoang, Phys. Rev. **D56**, 5851 (1997); Phys. Rev. **D56**, 7276 (1997). For QCD see: A. Czarnecki and K. Melnikov, Phys. Rev. Lett. **80**, 2531 (1998); M. Beneke, A. Signer and V.A. Smirnov, Phys. Rev. Lett. **80**, 2535 (1998).
- [22] S.N. Gupta and S.F. Radford, Phys. Rev. **D24**, 2309 (1981); ibid. **D25**, 3430 (1982).
- [23] S. Titard and F.J. Yndurain, Phys. Rev. **D49**, 6007 (1994).
- [24] H. Georgi, Nucl. Phys. **B361**, 339 (1991).
- [25] K. Melnikov and A. Yelkhovsky, Nucl. Phys. **B528**, 59 (1998).
- [26] A. H. Hoang, Phys. Rev. **D59**, 014039 (1999).
- [27] N. Brambilla, A. Pineda, J. Soto and A. Vairo, hep-ph/0002250.
- [28] K. Hasebe and Y. Sumino, hep-ph/9910424.
- [29] N. Van-Hieu and R. Faustov, Nucl. Phys. **53** 337 (1964).
- [30] Y.-Q. Chen, Y.-P. Kuang and R.J. Oakes, Phys. Rev. **D52**, 264 (1995).
- [31] M. Beneke, A. Signer and V. A. Smirnov, Phys. Lett. **B454**, 137 (1999).
- [32] M.L.G. Redhead, Proc. Roy. Soc. **A220** 219 (1953).
- [33] P.V. Nieuwenhuizen, Nucl. Phys. **B28** 429 (1971).
- [34] W. Buchmuller, Y. Ng, and S. Tye, Phys. Rev. **D24**, 3003 (1981); J. Pantaleone, S. Tye, and Y. Ng, Phys. Rev. **D33** 777 (1986).
- [35] A. H. Hoang, Phys. Rev. **D56**, 7276 (1997).
- [36] A. J. Buras and P. H. Weisz, Nucl. Phys. **B333**, 66 (1990).
- [37] M. J. Dugan and B. Grinstein, Phys. Lett. **B256**, 239 (1991).

- [38] S. Herrlich and U. Nierste, Nucl. Phys. **B455**, 39 (1995).
- [39] A. Manohar and I. Stewart, UCSD/PTH 00-05.
- [40] M. Luke and A.V. Manohar, Phys. Lett. **B286**, 348 (1992).
- [41] E. Eichten and B. Hill, Phys. Lett. B243 427 (1990), A. Falk, B. Grinstein, and M. Luke, Nucl. Phys. B357 185 (1991), B. Blok, J. Körner, D. Pirjol, and J. Rojas, Nucl. Phys. B496 358 (1997), C. Bauer and A. Manohar, Phys. Rev. D57 337 (1998).